Sandia National Laboratories

SAND2020-10249C

Residual uncertainty in processed line-of-sight returns from nacelle-mounted lidar due to spectral artifacts

Presented by:

Kenneth Brown and Thomas Herges

Wind Energy Technologies

Sandia National Laboratories

U.S. DEPARTMENT OF ENERGY NNSA

Sandia National Laboratories is a multimission laboratory managed and operated by National Technology & Engineering Solutions of Sandia, LLC, a wholly owned subsidiary of Honeywell International Inc., for the U.S. Department of Energy's National Nuclear Security Administration under contract DE-NA0003525.

SAND Number: SAND2020-6409 C

Introduction

Errors in lidar measurements stem both from the (1) line-of-sight velocity readings, v_{los}, themselves and (2) modeling approaches for reconstruction of the velocity vector

Topic of this presentation

Modern lidars show v_{los} biases ~≤ 0.2-m/s and std. dev. ~≤ 0.20-m/s [1] depending primarily on the inhomogeneities within the measurement volume (i.e. – turbulence, mean gradients, non-uniform backscatter)

Two largely unquantified sources of measurement error are embedded in the region of interest (ROI)

- Solid interference - due to solid returns from boresight or ground surface ⇒ bias error
- Amplitude noise - due primarily to shot noise in modern lidar [2], depends on the range-resolved intensity of the backscatter [3] ⇒ random error

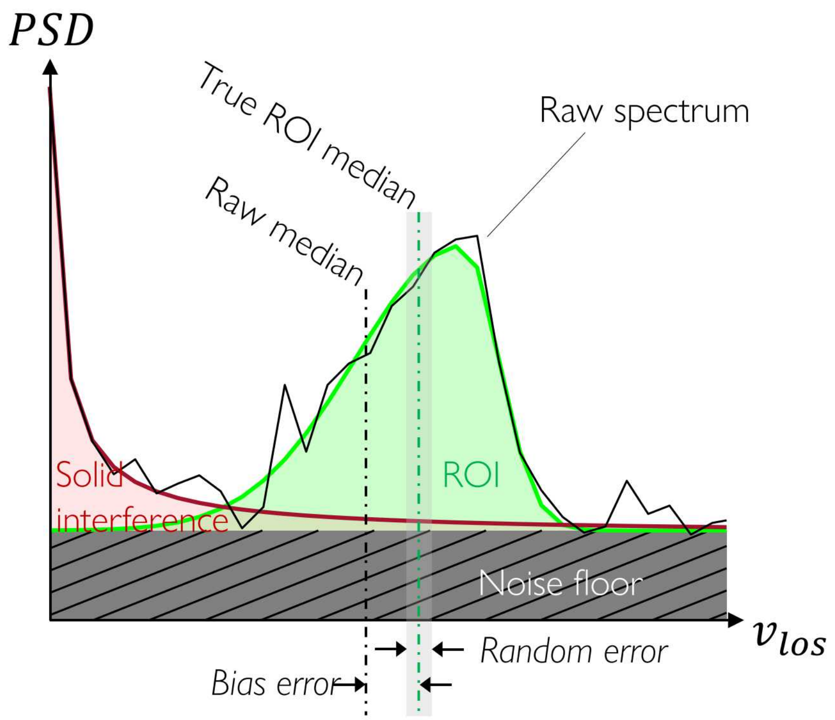

First line of attack toward reducing these errors is quality assurance/quality control (QAQC) processing

- Godwin *et al.* (2012) – bias correction vulnerable to a large degree of subjectivity in defining certain thresholds [4]
- Herges and Keyantuo (2019) – bias correction still partially subjective, bilateral filtering smooths amplitude fluctuations [5]

Methodology

Three-step process implemented to create uncertainty model

1. Generate a database of synthetic lidar spectra with known ground truth quantities of interest (QoIs) and artificial contamination

$m_{0_{ROI}}$, $m_{1_{ROI}}$, $m_{2_{ROI}}$, $m_{3_{ROI}}$, p_{solid}, σ_{noise} $\xrightarrow{\text{Shape param.}}$ Synthetic spectra generation $\xrightarrow{\text{Raw spectra}}$ $s = s_{ROI} + s_{solid} + s_{noise}$

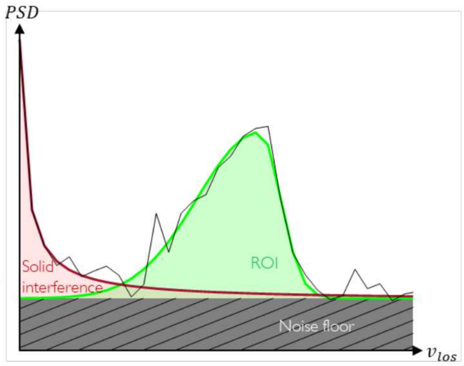

Scaled epsilon-skew-normal distribution [7]: $s_{ROI} = \frac{m_{0_{ROI}}}{m_{2_{ROI}}\sqrt{2\pi}} e^{-\frac{1}{2}\left(\frac{v_{los}-m_{1_{ROI}}}{m_{2_{ROI}}(1\mp m_{3_{ROI}})}\right)^2}$

Inverse function: $s_{solid} = \frac{p_{solid}}{1+(v_{los}-v_{solid})/w_{solid}}$

Randomized instances of noise (>400 per case): $s_{noise} = normrnd(0, \sigma_{noise})$ for each bin

Methodology

Three-step process implemented to create uncertainty model

1. Generate a database of synthetic lidar spectra with known ground truth quantities of interest (QoIs) and artificial contamination
2. Mimic data path of actual lidar returns by calculating QoIs with QAQC code

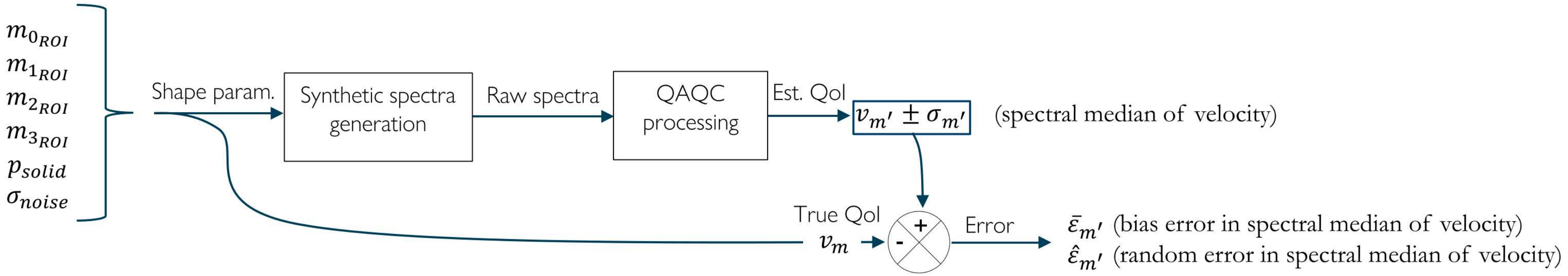

For any QoIs, we now have a database of the correspondence between the shape of the input spectra and any deviation in the output QoI from its original input value.

Methodology

Three-step process implemented to create uncertainty model

1. Generate a database of synthetic lidar spectra with known ground truth quantities of interest (QoIs) and artificial contamination
2. Mimic data path of actual lidar returns by calculating QoIs with QAQC code
3. Train models to produce *a posteriori* estimates of QoI uncertainty remaining after QAQC for any observed spectral shape

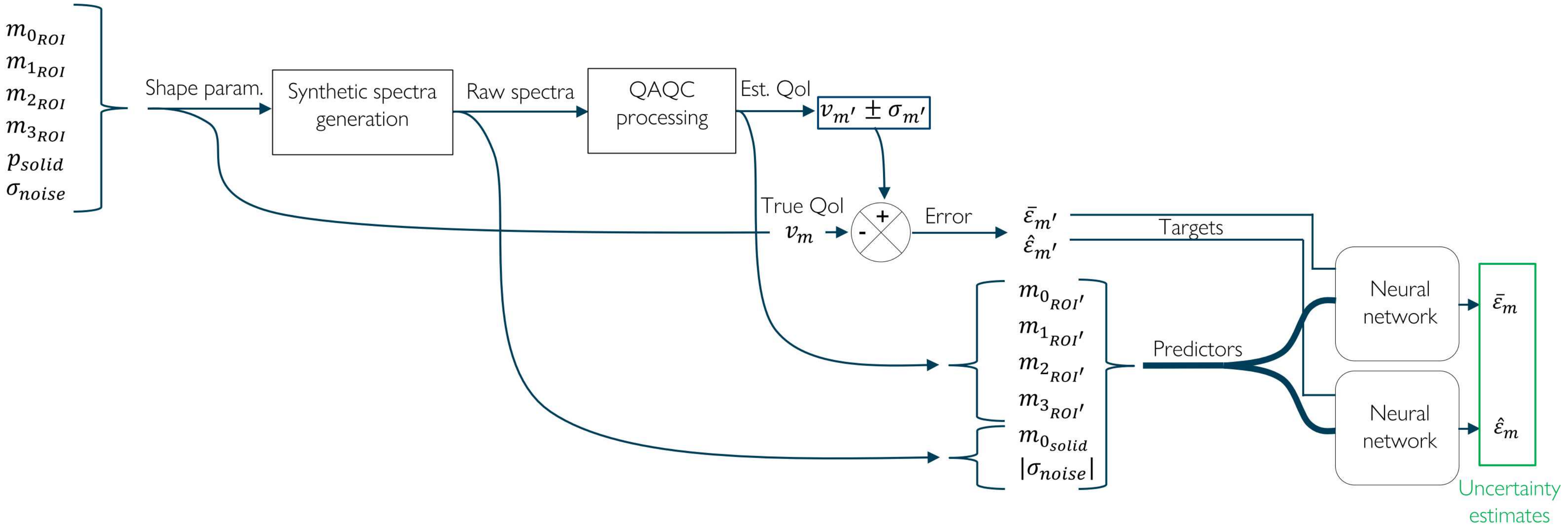

Methodology

Three-step process implemented to create uncertainty model

1. Generate a database of synthetic lidar spectra with known ground truth quantities of interest (QoIs) and artificial contamination
2. Mimic data path of actual lidar returns by calculating QoIs with QAQC code
3. Train models to produce *a posteriori* estimates of QoI uncertainty remaining after QAQC for any observed spectral shape

Supervised machine learning regression via neural networks:

- Architecture: two layers of perceptrons with 12 nodes each
- Transfer function: sigmoid symmetric
- Objective: mean-square error
- Algorithm: Levenberg-Marquardt
- Training cases: 800 – 2600; testing cases: 150 - 250

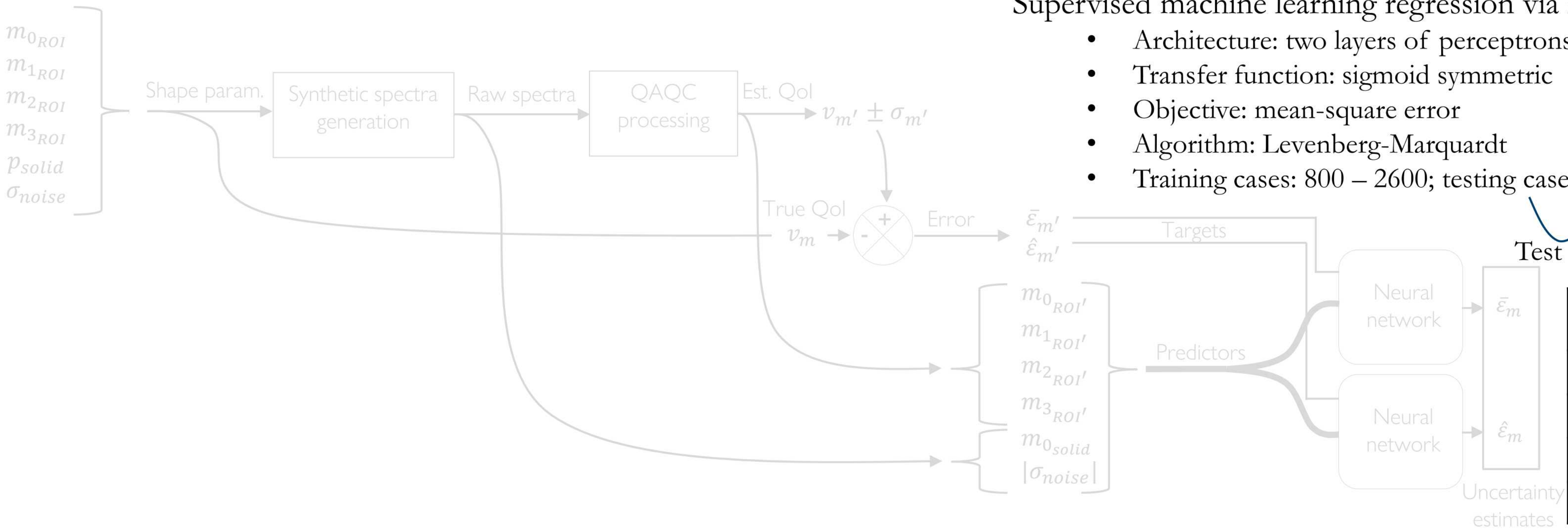

Test case error

Metric	*rms error* (m/s)
$\bar{\varepsilon}_m$	0.0129
$\bar{\varepsilon}_\sigma$	0.0245
$\hat{\varepsilon}_m$	0.00846
$\hat{\varepsilon}_\sigma$	0.00762

Experimental Setup

Facility

- Scaled Wind Farm Technology (SWiFT) facility in Lubbock, Texas, USA
  - Characterization of the atmospheric conditions in [8], recent benchmarking activities given in [9]

Lidar

- Continuous-wave DTU SpinnerLidar [10] rear-mounted on WTGa1
- Focus = 105 m from WTGa1 along the axis of the turbine rotor
- A rosette pattern is completed in 2 s and consists of 984 measurement locations, some below ground

Example Case

- Single scan taken in the morning of July 5, 2017 with $\overline{U}_{hub}$ = 6 m/s in an unstable ABL

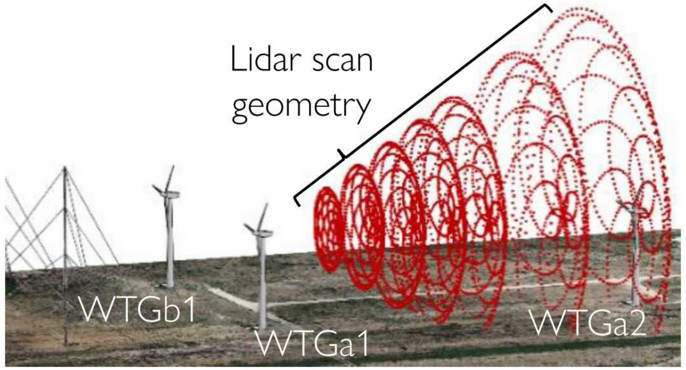

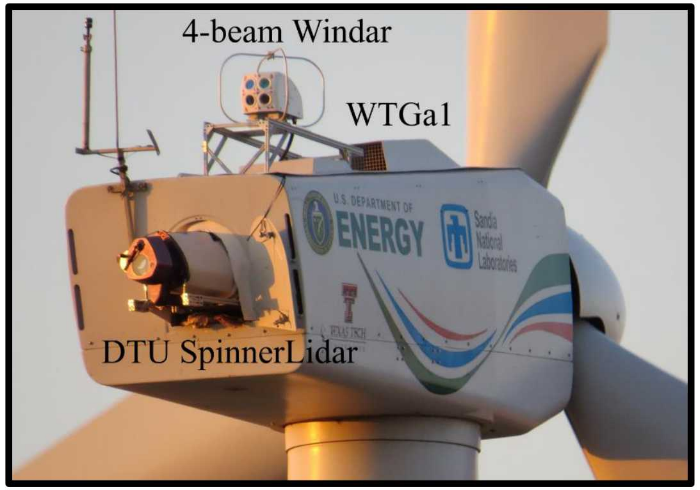

(Images from [9])

Results – Example Spectra

Rosette scan pattern of the 984 measurement locations with three selected spectra:

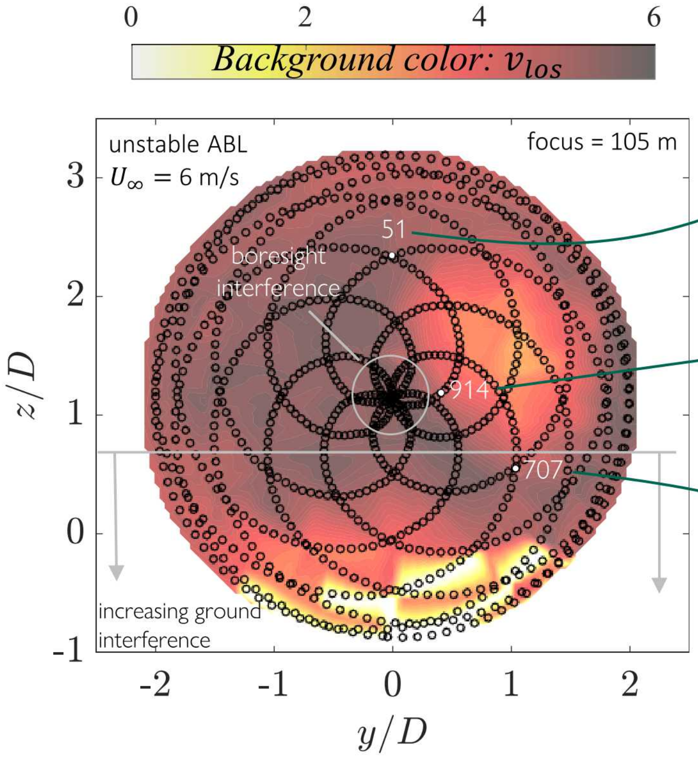

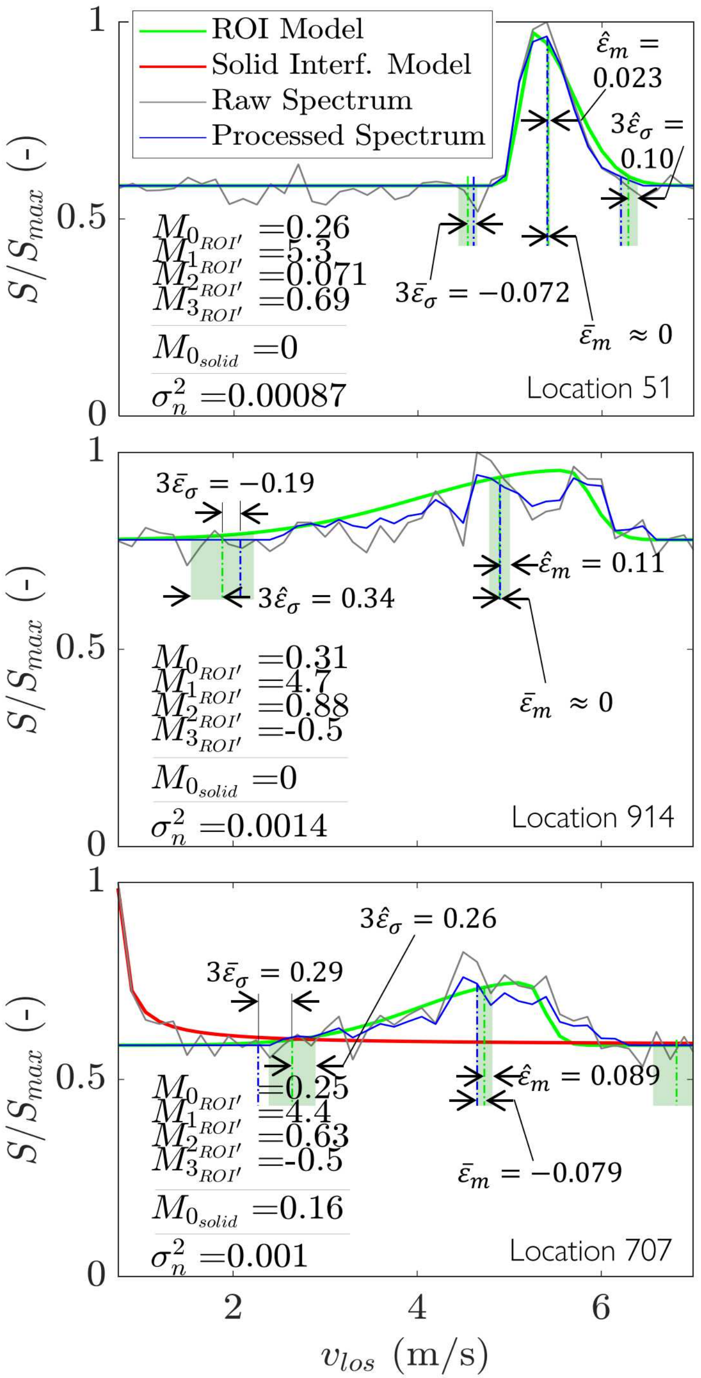

Results – Full-Field Error Maps

Bias error:

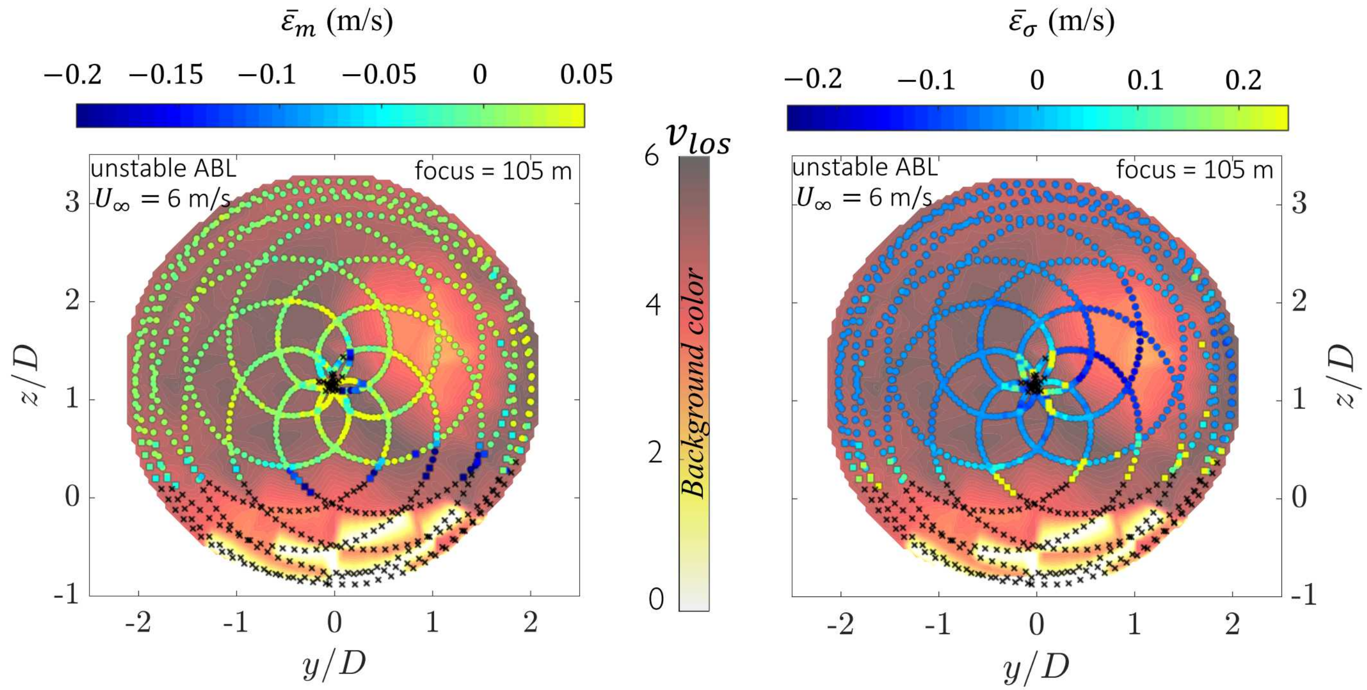

- Partial solid return magnitudes:
  - Ground: $\bar{\varepsilon}_m$ biases as negative as -0.62 m/s, or 13%
  - Boresight: $\bar{\varepsilon}_\sigma$ biases as negative as -0.18 m/s, or 6.6%
- Remainder of scan field: negligible bias (error magnitude < 0.05 m/s)
- Some unexpected scatter remains throughout the field, which suggests that the training of the error model could be refined

Results – Full-Field Error Maps

Random error (at 95% confidence):

Note:
Logarithmic scaling

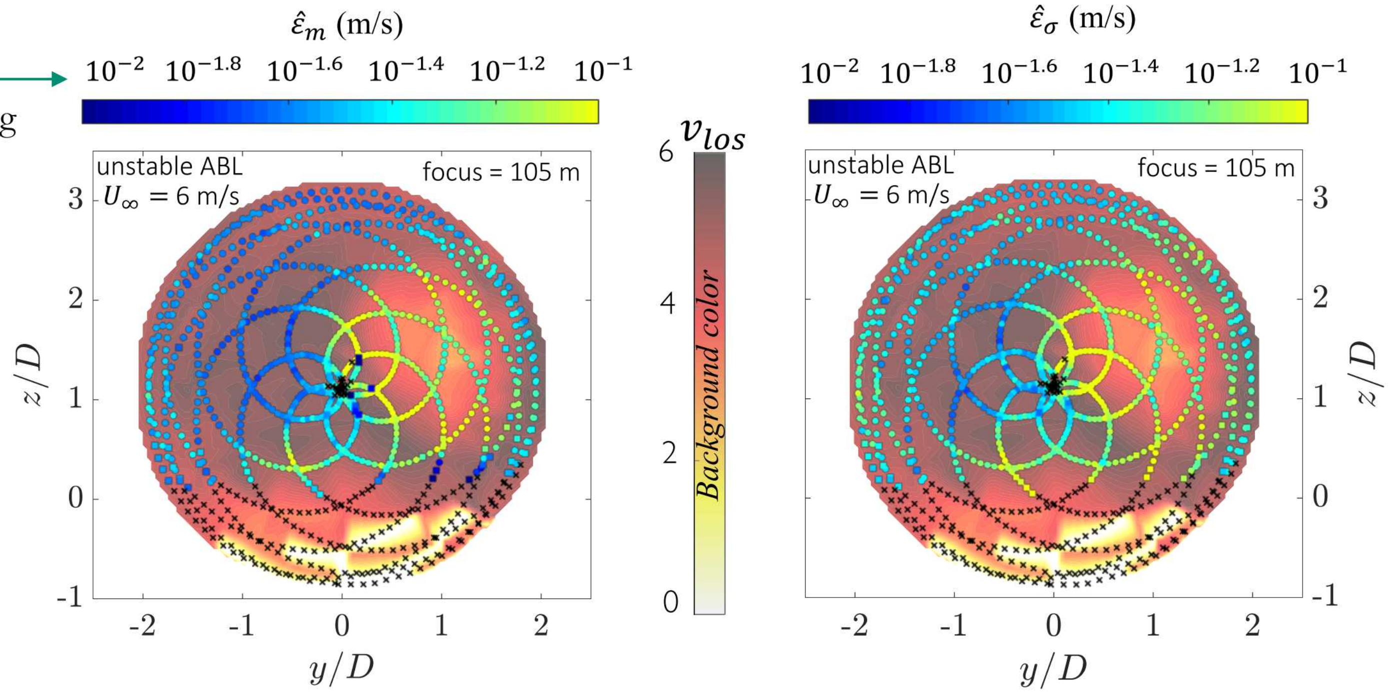

- As with the bias errors, random uncertainties are somewhat influenced by partial solid returns
- The more significant influence, however, is proximity to the wake region
  - $\hat{\varepsilon}_m$ maximum of $\pm$0.11 m/s ($\pm$2.5% of v_m)
  - $\hat{\varepsilon}_\sigma$ maximum $\pm$0.12 m/s ($\pm$13% of v_σ)

Results – Full-Field Error Maps

Random error (at 95% confidence):

Note:
Logarithmic scaling

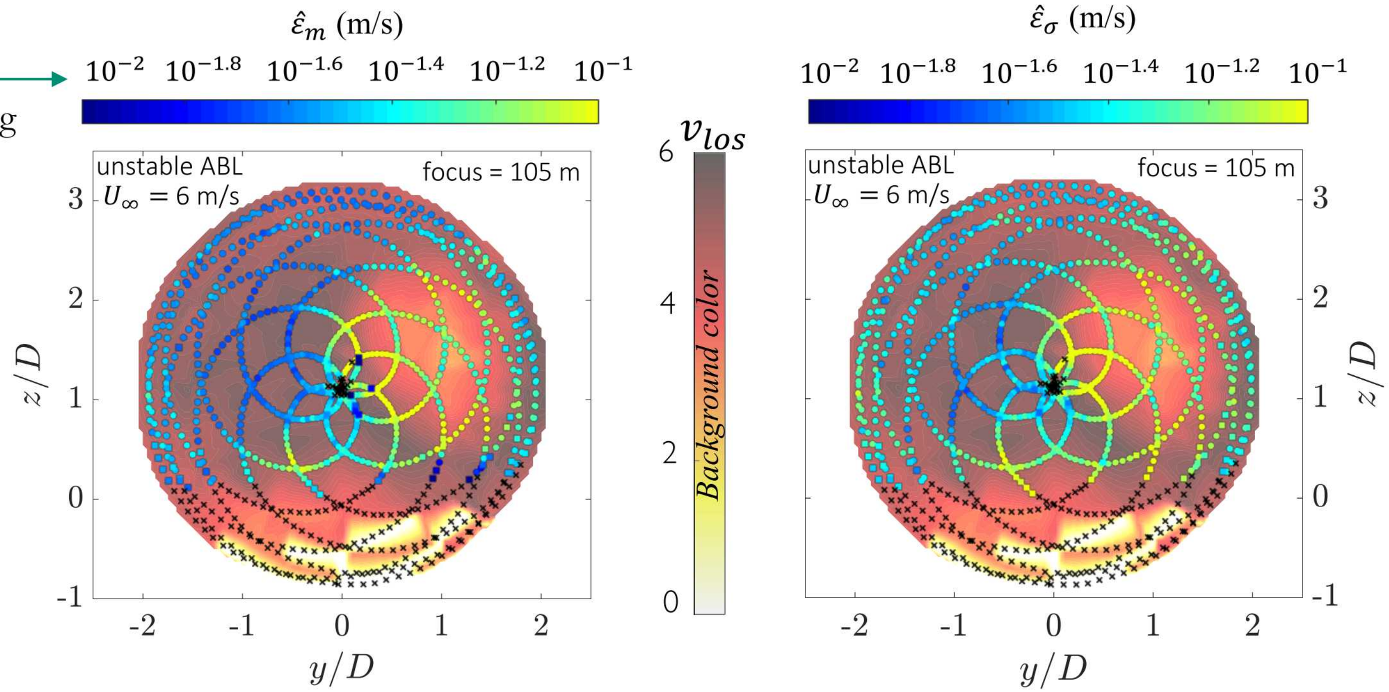

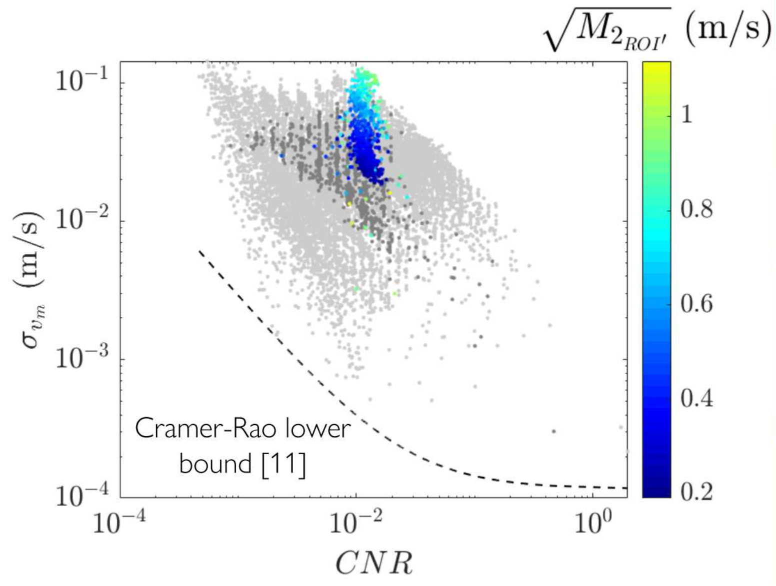

- As with the bias errors, random uncertainties are somewhat influenced by partial solid returns
- The more significant influence, however, is proximity to the wake region
  - $\hat{\varepsilon}_m$ maximum of $\pm$0.11 m/s ($\pm$2.5% of v_m)
  - $\hat{\varepsilon}_\sigma$ maximum $\pm$0.12 m/s ($\pm$13% of v_σ)

- Verification of the model versus theory

Conclusions and Future Work

New uncertainty quantification method developed leveraging machine learning (ML) for nacelle-mounted lidar

Uncertainty quantification is spatially dependent

- Bias correction for measurements pointed near ground/boresight $\leq$ 0.62 m/s (13%)
- Random uncertainties in the wake region up to $\pm$0.11 m/s ($\pm$2.5%) at 95% confidence

Ongoing work:

- Bypass QAQC code's QoI estimator and replace with ML

Thank you!

Sandia National Laboratories is a multimission laboratory
managed and operated by National Technology & Engineering Solutions
of Sandia, LLC, a wholly owned subsidiary of Honeywell International Inc.,
for the U.S. Department of Energy's National Nuclear Security Administration
under contract DE-NA0003525.

Sandia National Laboratories

References

1. **Courtney, M., R. Wagner, and P. Lindelöw**, *Testing and comparison of lidars for profile and turbulence measurements in wind energy*. IOP Conference Series: Earth and Environmental Science, 2008. **1.**
2. **Peña, A. and C.B. Hasager**, *Remote sensing for wind energy*. 2011.
3. **Liu, Z., et al.,** *Estimating random errors due to shot noise in backscatter lidar observations*. Applied optics, 2006. **45**(18): p. 4437-4447.
4. **Godwin, K., S. De Wekker, and G. Emmitt**, *Retrieving winds in the surface layer over land using an airborne Doppler lidar*. Journal of Atmospheric and Oceanic Technology, 2012. **29**(4): p. 487-499.
5. **Herges, T. and P. Keyantuo**. *Robust Lidar Data Processing and Quality Control Methods Developed for the SWiFT Wake Steering Experiment*. in Journal of Physics: Conference Series. 2019. IOP Publishing.
6. **Beresh, S.J.**, *Comparison of PIV data using multiple configurations and processing techniques*. Experiments in fluids, 2009. **47**(6): p. 883.
7. **Mudholkar, G.S. and A.D. Hutson**, *The epsilon–skew–normal distribution for analyzing near-normal data*. Journal of statistical planning and inference, 2000. **83**(2): p. 291-309.
8. **Kelley, C.L. and B.L. Ennis**, *SWiFT site atmospheric characterization*. 2016, Sandia National Lab.(SNL-NM), Albuquerque, NM (United States).
9. **Doubrawa, P., et al**., *Multimodel validation of single wakes in neutral and stratified atmospheric conditions.* Wind Energy, 2020.
10. **Mikkelsen, T., et al**., *A spinner-integrated wind lidar for enhanced wind turbine control.* Wind Energy, 2013. **16**(4): p. 625-643.
11. **Rye, Barry J., and R Michael Hardesty**. *Discrete spectral peak estimation in incoherent backscatter heterodyne lidar. I. Spectral accumulation and the Cramer-Rao lower bound.* IEEE transactions on geoscience and remote sensing 31.1 (1993): 16-27.